Advanced satellite image fusion techniques for estimating high resolution Land Surface Temperature time series

Mitraka Z., Chrysoulakis N.

Land Surface Temperature (LST) affects urban heat fluxes and is therefore its spatiotemporal patterns is a key parameter in urban microclimatic and energy budget studies. Although LST can be derived from satellite thermal measurements, currently there is no spaceborne instrument to provide frequent thermal imagery at high spatial resolution, which is essential for studying the urban microclimate. In this study, a synergistic algorithm that combines the frequent thermal measurements from Moderate Resolution Imaging Spectroradiometer (MODIS) with the high spatial resolution Landsat-8 imagery for estimating high spatial resolution LST is presented. The developed methodology was applied and high-resolution time series of LST for the case study of Heraklion, Greece were retrieved. The accuracy assessment performed by comparing the derived LST products with Advanced Spaceborne Thermal Emission and Reflection Radiometer (ASTER) LST products, indicated a good agreement.

Mitraka Z.[1,2*], Chrysoulakis N.[1]

1 Foundation for Research and Technology – Hellas, N. Plastira 100, 70013 Heraklion, Greece
2 Earth Observation Lab, University of Tor Vergata, Rome, Italy

***corresponding author e-mail: email: mitraka@iacm.forth.gr**

1 Introduction

Urban microclimate is strongly influenced by man-made structures and human activities and differs from that of the surrounding natural areas. One of the observed differences is that of Land Surface Temperature (LST) between the artificial and natural surfaces. LST is an important indicator for quantifying the surface urban heat islands, which is closely related to human comfort and cities energy use (Chrysoulakis et al. 2013).

Although LST can be derived by satellite thermal measurements, there is no spaceborne instrument to provide both frequent thermal imagery and at a high spatial resolution. The coarse spatial resolution or infrequent temporal coverage of the current and foreseen satellite thermal sensors limits the application of thermal infrared (TIR) remote sensing in urban environments. A spatial resolution of 50 or 100 m is the minimum requirement for urban thermal studies, because lower resolutions result in loss of detail for urban structures.

Landsat series of satellites retrieve TIR information in a resolution between 60 and 120 m, with the recently launched Landsat-8 that measures radiation in two thermal bands of 100 m spatial resolution. The Advanced Spaceborne Thermal Emission and Reflection Radiometer (ASTER) is a multispectral thermal instruments which measures in five TIR bands of 90 m spatial resolution (Gillespie et al. 1996). Although, these sensors provide TIR measurements of high spatial resolution, they have a low revisit rate (twice per month for Landsat 8 and much less for ASTER, limited also by cloud coverage). On the other hand, coarse spatial resolution instruments like the Moderate Resolution Imaging Spectroradiometer (MODIS), or the Advanced Very High Resolution Radiometer (AVHRR), provide daily TIR measurements of 1 km resolution. ESA's upcoming high spatial resolution mission, Sentinel-2, although it will have a great revisit rate of twice per week, it will not include a TIR sensor. Therefore, current and forthcoming TIR remote sensing is confronting the tradeoff between spatial and temporal resolution, and thus synergistic algorithms exploiting high resolution optical in information to disaggregate the coarse resolution TIR data has drawn the attention of the scientific community (Zhan et al. 2013).

In this study, a synergistic algorithm that unmixes the low-resolution TIR measurements from MODIS using the high spatial information from Landsat-8 imagery for estimating high spatial resolution LST is presented. The developed methodology was applied for the case study or Heraklion, Greece and high-resolution LST time series were derived for an 8-month period. The accuracy assessment of the performed by comparing the derived LST products with ASTER LST products.

2 Data and Methods

2.1 Case study and data

The methodology described below was applied to derive time series LST for the broader area of Heraklion, which is the larger city in the island of Crete, Greece. Heraklion is a rapidly growing urban area and is characterized by mixed land uses that include residential, commercial and industrial surfaces, transportation networks, agricultural surfaces and surfaces with natural vegetation. Fig. 1 shows the Urban Atlas (EEA 2010) land use map of the study area overlaid to Google Earth. The urban related surfaces are shown in blue, outlining the city core in the northern part of the study area, while agricultural related surfaces are shown in green. The industrial zone of Heraklion is located outside the main core in the central eastern part of the city.

A series of MODIS and Landsat-8 data were used for the estimation of the LST time series. Daily MODIS Level 1B (MOD021) data from both Terra and Aqua satellites for a period between April 1, 2013 and December 31, 2013 were acquired, along with all Landsat-8

images for the same time period. The Lansdat-8 acquisition dates are shown in Fig. 2. Only Landsat images with less than 50% cloud cover in the study site were used in the analysis and that is why there are some missing dates in Fig. 2. ASTER LST products were used to assess the accuracy of the MODIS-derived LST products. Three ASTER LST products were used to assess the accuracy of the derived LST products. ASTER data acquisition dates are shown in Fig. 2. The MODIS MOD05 product was also used to provide ancillary atmospheric information on water vapor and cloud cover. Finally, information included in the ASTER Spectral Library (SL) version 2.0 (Baldridge et al. 2009) was used for estimating emissivity.

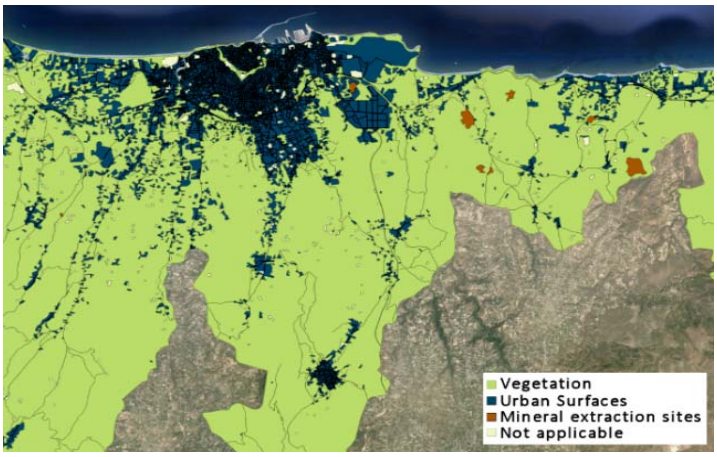

Fig. 1. The case study site, the city of Heraklion, Greece (Urban Atlas land use data overlaid to Google Earth).

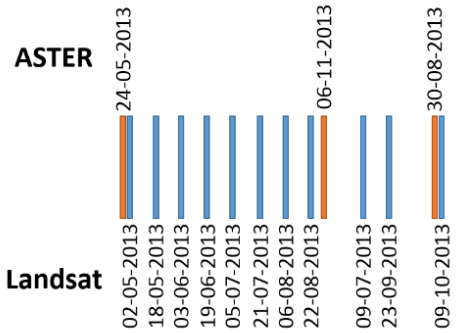

Fig. 2. Landsat-8 and ASTER acquisition dates. Blue lines represent Landsat-8 acquisitions and orange the ASTER ones. Missing dates correspond to cloudy scenes.

2.3 Methodology

The different steps of the methodology developed to derive time series of high spatial resolution LST is explained in this section. Information about the surface cover is estimated in high-resolution from Landsat-8 and it is updated for every acquisition. The surface cover information is then used to estimate emissivity using ancillary information from the ASTER SL, and also to enchase the spatial resolution of the MODIS TIR measurements. Resulting high-resolution emissivity and TIR measurements are combined with atmospheric information and high-resolution LST products are derived from a split-window algorithm.

The first step is to estimate and update surface cover abundance maps. This is done using linear spectral unmixing methods. Four fundamental surface cover types are assumed, i.e. vegetation, high-albedo Impervious, low-albedo impervious and soil. Image spectra, from the Landsat-8 images, are assigned to each cover type and are used as endmembers, to inverse the linear mixing problem for each pixel (Mitraka et al. 2012). Surface cover types abundance maps are derived and updated for every Landsat-8 scene.

To estimate high-resolution emissivity maps, emissivity values are assigned to each cover type, using samples form the ASTER SL corresponding to the study area. The mean value of selected samples for each surface cover is assumed representative for the surface type and the emissivity for each pixel is estimated assuming a linear relationship between the abundances and the representative emissivities (Mitraka et al. 2012).

Spatial-spectral unmixing is then used as per Mitraka et al. (2013) to enhance the spatial resolution of the low-resolution thermal bands. The contribution of land cover components is estimated for each low-resolution thermal pixel, by summing the estimated abundances. Each thermal pixel is then decomposed, using the contextual information of the neighboring pixels in a moving window:

$$\mathbf{E}^{(L)} = \min_{\mathbf{E}} \left\| \mathbf{S}^{(L)} - \mathbf{A}^{(L)} \cdot \mathbf{E}^{(L)} + a\frac{w^2}{n}\left(\mathbf{E}^{(L)} - \bar{\mathbf{S}}'^{(L)}\right) \right\|_2^2$$

where $\mathbf{S}^{(L)}$ is a vector of the thermal radiances of the pixels in the window $\boldsymbol{w}$, $\mathbf{A}^{(L)}$ is a matrix of the contributions of surface types, $\mathbf{E}^{(L)}$ is the thermal radiances under consideration, $\bar{\mathbf{S}}'^{(L)}$ are predefined spectra corresponding to each surface cover type and $\boldsymbol{a}$ is a regularization parameter to ensure that estimated spectra present small variations. High-resolution TIR bands are produced in this way for every MODIS acquisition, excluding pixels characterized as clouds in the respective MODIS water vapour product.

High spatial resolution LST is finally estimated using derived thermal information and the emissivity products in a split-window algorithm (Jimenez-Munoz and Sobrino 2008) compiling also information about water vapour from the MODIS water vapour product.

The accuracy of the proposed method was assessed by comparing the derived high-resolution LST maps to ASTER LST products (Gillespie et al. 1996). The ASTER sensor is on-board the Terra satellite, along with a MODIS sensor, and thus concurrent acquisitions were ideal for comparison. Accuracy was assessed for three available ASTER scenes (Fig. 2) and different error metrics were estimated.

3 Results and discussion

The described method was applied to the series of Landsat-8 and MODIS data and a time series of LST was derived for the case study. Pixels regarded as cloudy from either the Landsat or the MODIS products were accounted in the analysis. Fig. 3 shows the mean LST estimated for April to December 2013. Low-resolution pixels are outlined in the coastline area having extreme mean LST values. This is caused in the thermal radiation unmixing process due to sea influence. Thermal radiation measured by the low-resolution sensor is contaminated by sea emitted radiation. Problem could be possibly resolved by assuming also sea spectra in the unmixing process. It is worth noticing that the city of Heraklion is outlined in the mean LST image, implying an urban heat island effect for the study period.

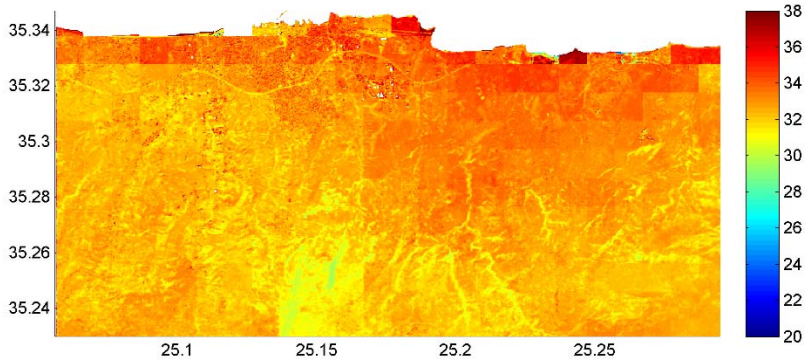

Fig. 3. Mean high-resolution LST time series for the period of April to December 2013.

The accuracy of the proposed method was assessed by comparing MODIS-derived LST products ($\boldsymbol{R_i}$) with the respective ASTER LST products ($\boldsymbol{S_i}$). Table 1 shows the error metrics estimated from the comparisons. In general, a good agreement is observed between estimated and LST and those of ASTER. Root mean Square Error (RMSE) lies around 2 K in the three cases, while the negative bias values indicate an overestimation of LST. The Mean Absolute Error (MAE) and Median Absolute Error (MdAE) indicate that the distribution of error in all cases lies around 1 K.

Table 1. Accuracy measures arose by comparing MODIS-derived LST to ASTER LST product.

Date	*RMSE*[1]	*Bias*[1]	*MAE*[1]	*MdAE*[1]
2013-04-24	1.8823	-0.3702	0.8049	1.9544
2013-06-11	2.3921	-0.4516	1.2330	1.2236
2013-08-30	2.0531	-0.1265	1.0047	1.9175

[1] $\boldsymbol{RMSE = \sqrt{mean(S_i - R_i)^2}}$, $\boldsymbol{bias = mean(S_i - R_i)}$, $\boldsymbol{MAE = mean(|S_i - R_i|)}$, $\boldsymbol{MdAE = median(|S_i - R_i|)}$

4 Conclusions

This study presented a method for retrieving high spatial resolution LST maps to be used for urban climate studies. Experimental results showed that this is capable of exploiting the frequent coverage of low-resolution thermal sensors and the high-resolution spatial information to derive LST. The proposed methodology can be applied to the upcoming ESA's Sentinel-2 and Sentinel-3 missions, which are expected to have a much higher revisit rate. Adjustments to improve the characterization of surface cover to account for the sea influence and also to better characterize daily changes can be proposed.

Acknowledgments The authors would like to thank the Jet Propulsion Laboratory and particularly Dr. Michael Abrams for kindly providing the ASTER images.

References

Baldridge a. M, Hook SJ, Grove CI, Rivera G (2009) The ASTER spectral library version 2.0. *Remote Sens Environ*. 113(4):711–715. doi:10.1016/j.rse.2008.11.007.

Chrysoulakis N, Lopes M, San José R, et al. (2013) Sustainable urban metabolism as a link between bio-physical sciences and urban planning: The BRIDGE project. Landsc Urban Plan. 112:100–117. doi:10.1016/j.landurbplan.2012.12.005.

Gillespie AR, Rokugawa S, Hook SJ, Matsunaga T, Kahle AB (1996) Temperature/emissivity separation Algorithm theoretical basis document, Version 2.3, JPL D-13916 Pasadena, CA: Jet Propulsion Lab.

EEA (2010). The GMES Urban Atlas. European Environment Agency, Copenhagen.

Jimenez-Munoz J-C, Sobrino JA. (2008) Split-Window Coefficients for Land Surface Temperature Retrieval From Low-Resolution Thermal Infrared Sensors. IEEE Geosci Remote Sens Lett.5(4):806–809. doi:10.1109 /LGRS.2008.2001636.

Mitraka Z, Berger M, Ruescas A, et al. (2013) Estimation of Land Surface emissivity and temperature based on spatial-spectral unmixing analysis. In: 3rd MERIS/(A)ATSR & OCLI-SLSTR Preparatory Workshop, Frascati, Italy, 15-19 October 2013.

Mitraka Z, Chrysoulakis N, Kamarianakis Y, Partsinevelos P, Tsouchlaraki A. (2012) Improving the estimation of urban surface emissivity based on sub-pixel classification of high resolution satellite imagery. Remote Sens Environ. 117:125–134. doi:10.1016/j.rse.2011.06.025.

Zhan W, Chen Y, Zhou J, et al. (2013) Disaggregation of remotely sensed land surface temperature: Literature survey, taxonomy, issues, and caveats. Remote Sens Environ. 131(19):119–139. doi:10.1016/j.rse.2012.12.014.